Oral Presentation

The 7th TSME International Conference on Mechanical Engineering
13-16 December 2016

TSME ICOME 2016
Mechanical Engineering Innovation for Green Society

AEC0013

Study on Co-Combustion of Pelletized and Moisturized Rice Husks in a Cone-Shaped Fluidized-Bed Combustor Using Fuel Staging for Reducing NO_x Emissions: Optimization of Operating Variables

Pichet Ninduangdee[1,*] and Vladimir I. Kuprianov[2]

[1] Division of Mechanical Engineering, Faculty of Industrial Technology, Phetchaburi Rajabhat University, Phetchaburi, 76000, Thailand
[2] School of Manufacturing Systems and Mechanical Engineering, Sirindhorn International Institute of Technology, Thammasat University, Pathum Thani, 12121, Thailand
[*] Corresponding Author: E-mail: ninduangdee.p@gmail.com, Tel.: +668 3 364 2438, Fax: +663 2 405 502

Abstract

This work was aimed at assessing the potential of fuel staging for reducing NO_x in a fluidized-bed combustor with conventional (bottom) air injection when co-firing rice husk pellets (as a base fuel) and moisturized rice husk (secondary fuel). The experiments were conducted at a fixed heat input to the reactor, ~200 kW_{th}, while ranging the energy fraction of the secondary fuel in the total fuel supply (EF_2) from 0 to 0.25, with excess air (EA) of 20% to 80% for each co-firing option. In a test run under fixed operating conditions, temperature and gas concentrations (O_2, CO, C_xH_y as CH_4, and NO_x as NO) were recorded along the combustor height, as well as at stack. The findings revealed important effects of EF_2 and EA on combustion and emission characteristics of the combustor. An optimization analysis was performed to determine optimal values of EF_2 and EA, leading to the minimal emission costs of the reactor. The best combustion and emission performance of the combustor is achievable when co-firing the pelletized and moisturized rice husks at $EF_2 \approx 0.15$ and EA ≈ 40%. With these optimal operating parameters, the combustor can be operated with high (~99%) combustion efficiency, while reducing the NO_x emissions by ~40%, as compared to firing the base fuel on its own, and controlling the CO and C_xH_y emissions at relatively low levels.

Keywords*:* Rice husks, fluidized-bed combustor, co-firing, fuel staging, NO_x reduction.

1. Introduction

Thailand is one of the world's largest rice exporters, producing some 35 million tons of paddy rice per year [1]. With high availability, rice husk (a residue from rice production) is an important bioenergy resource in this country. In 2014, the energy potential of rice husk in Thailand accounted for ~120 PJ [2].

A large number of research studies revealed that the fluidized-bed combustion systems (boilers, combustors) are highly suitable for converting rice husk into energy [3,4]. However, fluidized-bed combustion of rice husk is generally accompanied by elevated/high NO_x emissions. A level of the emissions from a system depends on the content of fuel-N, operating conditions (bed temperature and excess air), and a combustion method used [5–7].

Co-firing is a least-cost method that can effectively reduce NO_x emissions. As reported by related studies on grate-firing, pulverized fuel-firing, and fluidized-bed combustion techniques [8,9], co-firing is flexible for fuel type (coal, biomass, RDF, combustible wastes, etc.) and combustion techniques. Some recent studies revealed that co-firing of a biomass with relatively high calorific value and another one with higher moisture content and/or lower fuel-N in a fluidized-bed system can result in a significant reduction of NO_x emissions from the combustion system, whose level is dependent on mass/energy fractions of the co-fired biomass fuels and amount of excess air in the reactor [10,11].

A concept of fuel staging (biasing) in a combustion system with conventional (bottom) air injection has been previously proposed with the aim to reduce NO_x emissions [12]. In such a system, a base fuel (typically producing elevated NO_x when fired alone) is fed into the bottom region of a reactor together with all combustion air, and therefore burned in this region at excess air. Meantime, the rest part of the fuel (or a different fuel with dedicated properties) is delivered into the above zone with no air supply. A pioneering study on the co-firing of palm kernel shell (a base fuel) and empty fruit bunch in a fluidized-bed combustor using fuel staging at bottom air injection revealed a noticeable (35%) reduction of NO emission compared to burning palm kernel shell alone, mainly due to the formation of secondary peaks of CO and C_xH_y responsible for NO reduction in the vicinity of the secondary fuel injection. [13]. It was shown that an extent of the NO emission reduction depended on the energy share of the co-fired fuels and excess air. However, as follows from the literature review, limited attention has been paid to biomass–biomass co-firing with fuel staging in fluidized-bed combustion systems.

This study was aimed at assessing a potential of NO_x reduction in a fluidized-bed combustor via the use of fuel staging (at bottom air injection) when co-firing two types of rice husk with different fuel properties. Effects of fuel staging (mass/energy fraction of the co-fired fuels in the total fuel supply) and excess air on the behavior of O_2, CO, C_xH_y (as CH_4), and NO_x (as

Table 1 Ultimate and proximate analyses, and the lower heating value (all on an as-fired basis) of the selected fuels used in (co-)firing tests

Property	Pelletized rice husk	Moisturized rice husk
Proximate analysis (wt.%)		
Moisture	9.8	29.6
Volatile mater	64.9	41.9
Fixed carbon	15.4	14.3
Ash	9.9	14.2
Ultimate analysis (wt.%)		
C	43.27	29.94
H	5.04	3.01
O	31.17	22.93
N	0.79	0.34
S	0.02	0.01
Lower heating value (kJ/kg)	15,100	10,600

NO) inside the combustor, as well as on the major gaseous emissions (CO, C_xH_y, and NO_x) and combustion efficiency of the reactor, were investigated. Optimization of excess air and energy fraction of the secondary fuel was among the objectives of this work.

2. Materials and Methods

2.1 The fuels and bed material

In this work, pelletized rice husk (PRH) was used as a base (or primary) fuel, whereas moisturized rice husk (MRH) was selected as secondary fuel in co-firing experiments. The pellets of the base fuels had a cylindrical shape with a diameter of 6 mm and a variable length of 5–15 mm, whereas the average dimensions of MRH particles were 2-mm width, 0.5-mm thickness, and 10-mm length. Prior to experiments, MRH was prepared by adding a specified amount of water to "as-received" rice husk.

The proximate and ultimate analyses, and the lower heating value of the selected biomass fuels are presented in Table 1. It can be seen in Table 1 that the calorific value of MRH was substantially lower than that of PRH, mainly due to the higher fuel-moisture content in MRH. All issues related to formation and emission of SO_2 were omitted from this study because of insignificant fuel-S content in both fuels.

Typically, rice husk ash includes 85–95% SiO_2 and 1.5–2.5% K_2O at insignificant contents of other elements [14]. Therefore, rice husk displays no propensity for bed agglomeration [15]. For this reason, a conventional bed material, silica sand of the 2500 kg/m^3 solid density and 0.3–0.5 mm in particle sizes, and containing 88% SiO_2 (by wt.), was used as the bed material in the combustor during PRH/MRH co-firing. In all tests, the (static) bed height was fixed at 30 cm.

2.2 Experimental facilities

Fig. 1 shows the schematic diagram of a cone-shaped fluidized-bed combustor (referred to as 'conical FBC'). A detailed description of the combustor configuration has been provided in previous studies on individual firing of various biomass fuels [16,17]. However, to perform the co-firing experiments with fuel staging, the combustor was modified prior to this work, i.e., equipped with an additional screw-type fuel feeder to supply the secondary fuel into the reactor. The primary fuel was injected into the conical section of the combustor at 0.65 m above the air distributor, whereas the secondary fuel was delivered into the cylindrical section 0.5 m higher, as shown in Fig. 1.

Apart from the conical FBC (equipped with a bubble-cap air distributor), the experimental set up included an air blower, two screw-type fuel feeders, a cyclone collecting particulate matter generated during the fuels co-firing, a diesel-fired start-up burner, as well as facilities for data acquisition and treatment.

2.3 Experimental methods

Two groups of experimental tests, for (1) conventional combustion of PRH and (2) co-firing of PRH and MRH using fuel staging at bottom air injection, were performed on the conical FBC at an identical (~200 kW_{th}) heat input to the reactor. To ensure this heat input, PRH and MRH were delivered into the reactor at the feed rates of $\dot{m}_{f1}$ and $\dot{m}_{f2}$, respectively. In this work, the energy fraction of the secondary fuel in the total fuel supply (EF_2) and the percent excess air (EA) were selected as independent operating parameters. Note that EF_2 was determined as a ratio of the energy share by MRH ($\dot{m}_{f2}LHV_{f2}$) to the total heat input to the reactor by the two fuels, ($\dot{m}_{f1}LHV_{f1}+\dot{m}_{f2}LHV_{f2}$).

At a first stage of this work, PRH was co-fired with MRH at three values of EF_2 (0, 0.15, and 0.25) for two specified amounts of excess air, 40% and 80%,

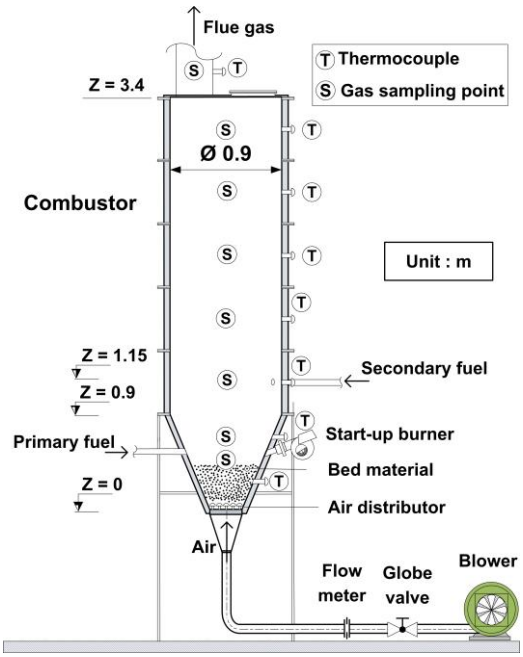

Fig. 1 Schematic diagram of the conical FBC for co-firing tests using fuel staging at bottom air supply

to investigate the effects of fuel staging and excess air on formation and oxidation/reduction of the major gaseous pollutants inside the reactor. During a test run at fixed EF_2 and EA, temperature, O_2, CO, C_xH_y (as CH_4), and NO_x (as NO) were measured along the reactor centerline and at the cyclone exit, using a "Testo-350" gas analyzer.

To investigate effects of the operating parameters on the emissions and combustion efficiency of the conical FBC, another (enhanced) test group was performed for five values of EF_2 (0, 0.1, 0.15, 0.2, and 0.25), at four specified EA (20%, 40%, 60%, and 80%) for each co-firing option. In test runs of this group, the CO, C_xH_y (as CH_4), and NO emission concentrations were measured along with O_2 at stack.

For each test run, the actual amount of (total) EA was quantified by using O_2, CO and C_xH_y (as CH_4) measured at stack [18]. The combustion-related heat losses of the conical FBC were estimated according to Ref. [18] based on a concept of 'equivalent fuel', whose properties were determined as the weighted averages (by taking into account the corresponding properties and the mass fractions of PRH and MRH). The combustion efficiency of the combustor was then predicted by subtracting the heat losses from 100%.

2.4 Models for optimization of operating conditions

To determine the optimal values of EF_2 and EA ensuring the minimum "external" (emission) costs of the co-firing PRH and MRH using fuel staging, a "cost-based" optimization method was employed in this work [17,19]. As the reactor was operated at constant heat input, the effect of CO_2 on the emission costs was omitted in this analysis.

An objective function used for the optimization of EF_2 and EA was therefore represented as:

$$J_{ec} = \mathrm{Min}(P_{NOx}\dot{m}_{NOx} + P_{CO}\dot{m}_{CO} + P_{CxHy}\dot{m}_{CxHy}) \quad (1)$$

In this study, the specific emission costs of NO_x (as NO_2) and C_xH_y (as CH_4) were assumed as P_{NOx} = 2400 US$/t and P_{CH4} = 330 US$/t, respectively, according to Ref. [20]. However, limited data regarding the specific CO emission cost, P_{CO}, is available. As reported in a related study, the ratio of P_{NOx} to P_{CO} is generally ranged from 5 to 8 [21]. So, it was decided to assume P_{CO} = 400 US$/t in this optimization analysis.

In Eq. (1), the emission rates of NO_x (as NO_2), CO, and C_xH_y (as CH_4) were determined, by taking into account the fuel feed rates of the co-fired fuels (kg/s) and actual pollutant concentrations (ppm) at stack, as:

$$\dot{m}_{NO_x} = 2.05\times10^{-6}(\dot{m}_{f1}+\dot{m}_{f2})NO_x V_{dg,cf} \quad (2)$$

$$\dot{m}_{CO} = 1.25\times10^{-6}(\dot{m}_{f1}+\dot{m}_{f2})CO V_{dg,cf} \quad (3)$$

$$\dot{m}_{C_xH_y} = 0.71\times10^{-6}(\dot{m}_{f1}+\dot{m}_{f2})C_xH_y V_{dg,cf} \quad (4)$$

where V_{dg} (Nm^3/kg-fuel) is the volume of dry flue gas at actual EA estimated according to Ref. [18].

3. Results and Discussion

3.1 Behavior of temperature and O_2 in the reactor

Fig. 2 compares the axial profiles of temperature

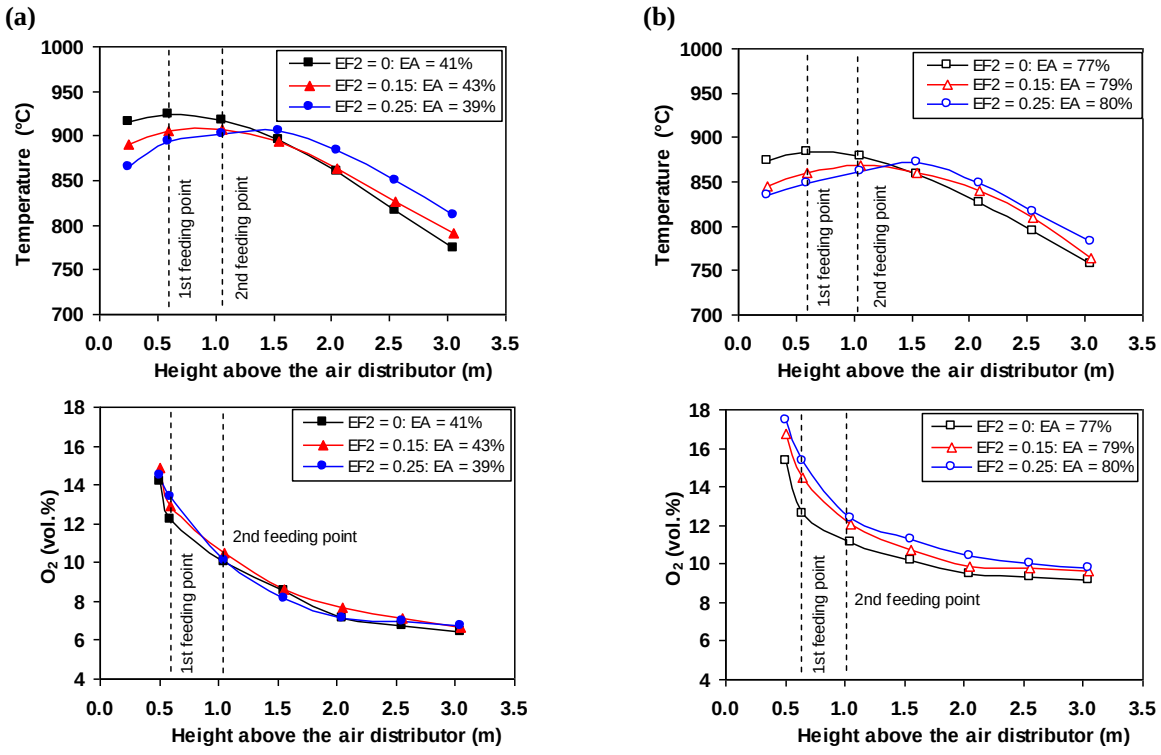

Fig. 2 Effects of the energy fraction of the secondary fuel (EF_2) on the axial profiles of temperature and O_2 in the conical FBC co-fired with PRH and MRH using fuel staging at excess air (EA) values of (a) ~40% and (b) 80%

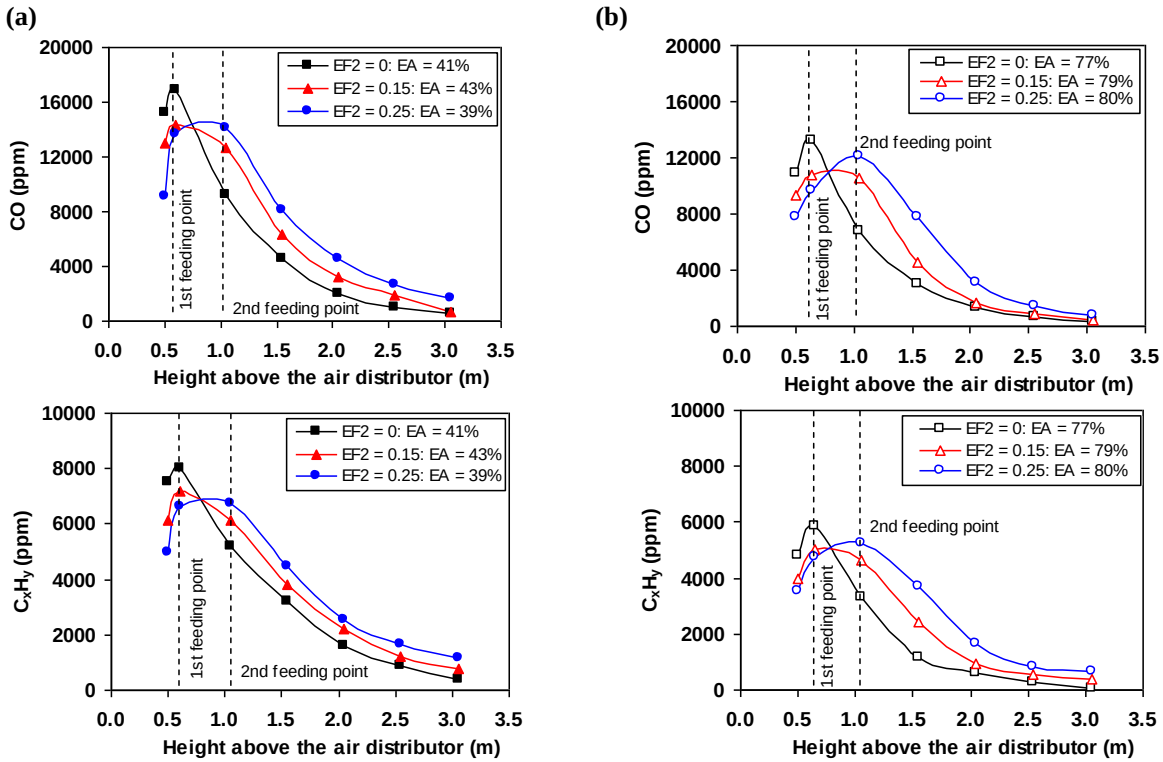

Fig. 3 Effects of the energy fraction of the secondary fuel (EF_2) on the axial profiles of CO and C_xH_y in the conical FBC co-fired with PRH and MRH using fuel staging at excess air (EA) values of about (a) 40% and (b) 80%

and O_2 in the combustor between the co-firing options at different EF_2 for two EA values (~40% and ~80%). From Fig. 2, the energy fraction of the secondary fuel (MRH), or fuel biasing, had noticeable effects on both temperature and O_2 at different points inside the reactor.

As seen in Fig. 2, the axial profiles of temperature were fairly uniform in all test runs, exhibiting, however, a slight positive gradient in the bottom region of the combustor and a negative gradient in the upper regions. The positive gradient was likely due to the effects of (i) combustion air injected through the air distributor at the ambient temperature and (ii) endothermic devolatilization of PRH (in the vicinity of primary fuel injection). However, the negative gradient was mainly caused by the heat loss across the combustor walls. With increasing EF_2 (at fixed EA), the temperature at all points within the bottom region (including the temperature peak) decreased, mainly due to (i) the reduced feed rate of the primary fuel (leading to a local raise in the excess air ratio) and (ii) lowered heat release in this region. In the meantime, an increase in EF_2 resulted in shifting the location of the temperature peak from Z = 0.6 m (i.e., from the level of PRH injection) to Z = 1.6 m, i.e., somewhat above the level of MRH injection.

With increasing EA (at fixed EF_2), the local temperature at all points inside the combustor dropped by 50–60 °C. This fact can be explained by the dilution effects of excessive air.

It can be seen in Fig. 2 that in all test runs, O_2 diminished gradually along the reactor height, showing, however, a minor influence of EF_2. A substantial axial gradient of O_2 was observed in a lower part of the reactor (Z < 1.6 m), comprising primary and secondary combustion zones, whereas in the upper part, the O_2 consumption (and, accordingly, fuel oxidation) along the reactor height occurred with an insignificant rate.

With increasing EA, O_2 at all points inside the conical FBC was higher, primarily due to a greater amount of air supplied into the combustor.

3.2 Formation and oxidation of CO and C_xH_y in the conical FBC

Fig. 3 shows the axial profiles of CO and C_xH_y (as CH_4) in the conical FBC for the same operating parameters as in Fig. 2. For all experiments, these profiles exhibited two specific regions, pointing at the rapid (net) formation of the pollutants in the bottom region of the conical FBC, and (on the contrary) at the high rate of CO and C_xH_y oxidation in the upper region (cylindrical section) of the reactor.

In the bottom region, CO and C_xH_y (generally originated from biomass volatile matter) showed a rapid increase along the reactor height, mainly due to the prompt devolatilization of the primary fuel. Due to the breakdown and further oxidation of C_xH_y to CO (under high-temperature conditions), CO at different points along the reactor height was substantially higher than C_xH_y. Nevertheless, the rate of C_xH_y generation at the combustor bottom was apparently higher than that of C_xH_y decomposition. In this region, CO was then oxidized to CO_2 [22], mainly via the reactions involving O and OH radicals, however at a rate substantially lower than that of CO formation.

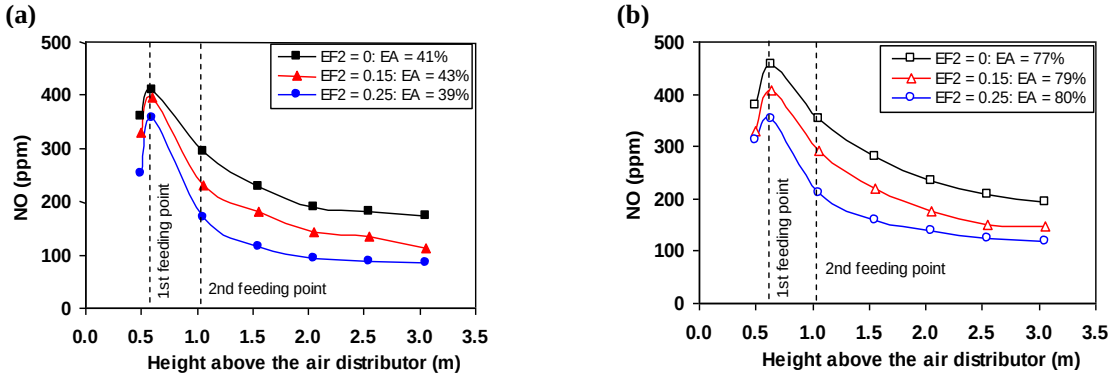

Fig. 4 Effects of the energy fraction of the secondary fuel (EF_2) on the axial profiles of NO in the conical FBC co-fired with PRH and MRH using fuel staging at excess air (EA) values of about (a) 40% and (b) 80%

With increasing EF_2 (at fixed total EA), both CO and C_xH_y decreased in the bottom region, mainly due to the above-mentioned increase of the local excess air ratio that enhanced the CO and C_xH_y oxidation rates. However, the peaks of C_xH_y and CO were shifted into the secondary combustion zone, generally due to the rapid devolatilization of MRH in the vicinity of fuel injection. Due to this fact, CO and C_xH_y at all points in the reactor's cylindrical section were higher than those during individual combustion of PRH, the stronger effects being observed at higher EF_2.

It can be further noticed that, compared to the conventional combustion, the fuel staging extended the region with high concentrations of CO and C_xH_y, covering the secondary combustion zone, thus creating the conditions for reducing a part of NO (formed in combustion of PRH in the reactor's conical section) to N_2 in the secondary combustion zone.

In the region above the MRH injection, where the rates of decomposition/oxidation reactions prevailed those of primary (formation) processes and reactions, both CO and C_xH_y decreased rapidly along the reactor height to their minimums at the reactor top. As seen in Fig. 3, after switching excess air to a higher level, both CO and C_xH_y significantly decreased at all points in reactor's cylindrical section, basically due to the enhanced oxidation rates of the two pollutants.

3.3 Formation and reduction of NO in the reactor

In all trials, the concentration of NO_2 in NO_x was negligible. In the below analysis, NO_x is therefore represented by NO.

Like CO and C_xH_y, NO originated generally from biomass volatile matter, via oxidation of volatile NH_3

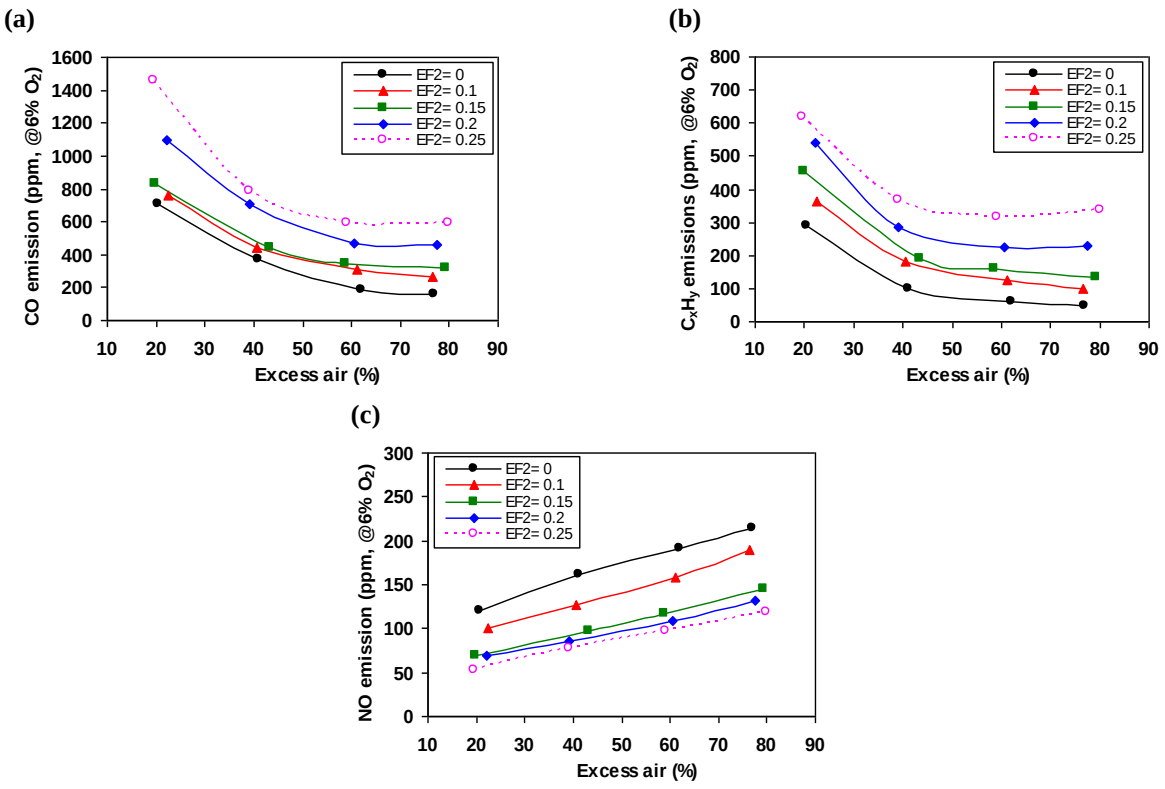

Fig. 5 Emissions of (a) CO, (b) C_xH_y (as CH_4), and (c) NO from the conical FBC when co-firing PRH and MRH at variable operating parameters (EF_2 and EA)

and HCN in multiple routes of the fuel-NO formation mechanism (including the proportional effects of fuel-N, excess air, and temperature) [5]. However, due to some secondary reactions, such as catalytic reduction of NO by CO (on the surface of fuel char/ash particles) and homogeneous reactions of NO with light C_xH_y and NH_2/NH radicals, NO formed in the primary reactions was reduced to a substantial extent [5,23].

Fig 4 depicts the axial profiles of NO in the conical FBC for the same co-firing options (EF_2) and operating conditions as in Figs. 2 and 3. Similar to CO and C_xH_y, all axial NO profiles showed two specific regions in the combustor, as seen in Fig. 4. In the first (lower) region (Z < 0.6 m), where the rate of the NO formation reactions was significantly higher than that of the NO reduction reactions, NO increased rapidly along the combustor height, attaining the NO peak at Z = 0.6 m (i.e., at the level of PRH feeding) in all test runs. With increasing EF_2, the NO peak at this point somewhat decreased despite the above-mentioned increase of the excess air ratio in the bottom region. This result can be likely attributed to the lowered bed temperature (see Fig. 2) and higher CO and C_xH_y in this zone (see Fig. 3).

In the upper regions (Z > 0.6 m), the rate of reactions responsible for the NO reduction prevailed that of NO formation, which led to a gradual decrease of NO along the reactor height. However, as seen in Fig. 4, with increasing EF_2, the NO reduction rate at 0.6 m < Z < 1.5 m was noticeably higher than that at the combustor top, particularly at the highest feeding rate of MRH (i.e., at EF_2 = 0.25). This fact can be attributed to the relatively high concentrations of CO and C_xH_y in the vicinity of secondary fuel injection, which enhanced the catalytic reduction of NO in this zone. Therefore, in the test at EF_2 = 0.25 (at fixed EA), NO at all points inside the combustor was lowered, as compared to the tests at EF_2 = 0 and EF_2 = 0.15.

3.4 Emissions

Fig. 5 depicts the CO, C_xH_y (as CH_4), and NO emissions from the conical FBC (all on a dry gas basis and at 6% O_2) when (co-)firing PRH and MRH at variable EF_2 and EA. It can be seen in Fig. 5 that in all test runs with fuel staging, the CO and C_xH_y emissions from the combustor were higher compared to burning PRH alone, following the specifics in formation and oxidation of these pollutants in different regions inside the reactor. With increasing EA from ~20% to ~40% (at fixed EF_2), both emissions decreased significantly, showing, however, rather weak effects of this operating parameter at its higher values (60–80%).

Table 2 Predicted heat loss and combustion efficiency of the conical FBC co-fired with PRH and MRH for variable excess air (or O_2 at stack) and energy fraction of moisturized rice husk in the total fuel supply (EF_2)

Excess air (%)	Energy fraction of MRH (EF_2)	O_2 at the cyclone exit (vol.%)	Unburned carbon in PM (wt.%)	CO[a] (ppm)	C_xH_y[a] (ppm)	Heat loss (%) due to:		Combustion efficiency (%)
						unburned carbon	incomplete combustion	
Conventional combustion of PRH								
21	0	3.7	3.63	709	290	0.81	0.74	98.4
41		6.2	3.15	373	98	0.70	0.31	99.0
62		8.1	2.09	184	61	0.46	0.17	99.4
77		9.1	1.98	158	46	0.44	0.14	99.4
Co-firing PRH and MRH using fuel staging								
22	0.1	4.0	1.47	759	364	0.36	0.86	98.8
41		6.1	2.89	440	180	0.71	0.45	98.8
61		8.0	3.02	311	125	0.74	0.32	98.9
77		9.1	2.89	265	101	0.71	0.26	99.0
20	0.15	3.7	2.12	835	455	0.54	1.03	98.4
43		6.4	2.49	440	192	0.64	0.48	98.9
59		7.8	2.51	347	160	0.64	0.39	99.0
79		9.3	2.30	317	134	0.59	0.34	99.1
22	0.2	4.0	2.93	1099	542	0.78	1.24	98.0
39		6.0	2.36	704	285	0.63	0.71	98.7
61		8.0	2.45	473	225	0.65	0.52	98.8
77		9.2	2.29	460	228	0.61	0.52	98.9
20	0.25	3.7	2.09	1463	618	0.58	1.51	97.9
39		6.0	1.96	783	368	0.54	0.86	98.6
59		7.9	2.13	595	317	0.59	0.70	98.7
80		9.4	2.33	593	337	0.65	0.73	98.6

[a] At 6% O_2 on dry gas basis.

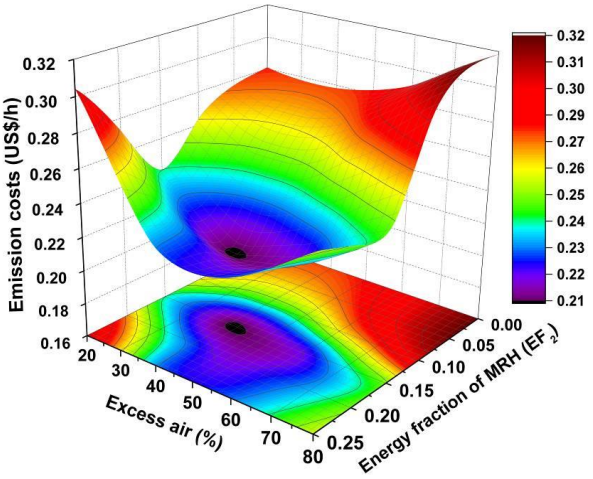

Fig. 6 Effects of the energy fraction of MRH and excess air on the emission costs of in the conical FBC using fuel staging during co-firing PRH and MRH

On the contrary, at fixed EA, the fuel staging resulted in the lower NO emission compared to burning of PRH on its own, and the NO emission reduction was more significant with increasing EF_2. This result can be generally attributed to the elevated CO and C_xH_y in the secondary combustion zone and upper regions (discussed previously), which enhanced the catalytic reduction of NO in the cylindrical section of the reactor. However, with increasing EA (for each fuel option), the NO emission increased, following the fuel-NO formation mechanism.

3.5 Combustion efficiency

Table 2 presents the predicted heat loss due to unburned carbon and that due to incomplete combustion together with the combustion efficiency of the conical FBC co-fired with PRH and MRH at different EF_2 and (actual) values of EA (or O_2 at stack). Table 2 also includes some supporting variables, such as the unburned carbon content in PM and the CO and C_xH_y emissions, required for predicting the heat losses.

As seen in Table 2, when firing pure PRH, the unburned carbon content in PM decreased as EA was increased, pointing at the enhanced rate of char-C burnout with higher excessive air. However, when using fuel staging, the impacts of EF_2 and EA on the unburned carbon were rather weak.

From Table 2, EF_2 and EA showed substantial effects on the CO and C_xH_y emissions, and, therefore, on the heat loss due to incomplete combustion. An increase in EA (at any fixed EF_2) led to a significant decrease of this heat loss. This result was generally due to the enhanced rate of the CO and C_xH_y oxidation in different regions inside the reactor. On the contrary, with increasing EF_2 (at fixed EA), the heat loss due to incomplete combustion increased, which resulted in some reduction of the combustion efficiency.

3.6 Optimal operating parameters

Fig. 6 depicts the 3-D surface representing the emission costs of the (co-)firing PRH and MRH in the selected combustor using fuel staging (at bottom air injection), which was obtained using Eqs. (1)–(4) and the above-reported CO, C_xH_y, and NO emissions, along with other relevant parameters, all quantified for the ranges of EF_2 and EA.

It can be seen in Fig. 6 that EF_2 and EA had substantial influences on the emission costs. With increasing EF_2 at relatively low EA, the "external" costs increased to a significant level, generally due to contributions of the CO and C_xH_y emissions to the total emission costs. On the contrary, an impact of NO on the 3-D surface was substantial when co-firing the selected biomass fuels at low values of EF_2 and relatively high EA.

From Fig. 6, the emission costs were minimal for the co-firing of PRH and MRH at $EF_2 \approx 0.15$ and EA ≈ 40%. Under these optimal operating conditions, the reactor can be operated with high (~99%) combustion efficiency, while reducing the NO_x emissions by ~40%, as compared to firing the base fuel on its own, and controlling the CO and C_xH_y emissions at relatively low levels.

Thus, fuel-staged co-combustion of PRH and MRH using bottom air supply exhibits a potential for NO emission reduction from the conical FBC, and no adverse effects on the combustor's operation.

4. Conclusions

The effects of fuel staging on the emissions and combustion efficiency of a conical fluidized-bed combustor co-fired with rice husk pellets (used as a base fuel) and moisturized rice husk (secondary fuel), injected into the reactor at different levels, have been investigated for variable energy fraction of moisturized rice husk (in total fuel supply) and excess air.

When using fuel staging at a conventional (bottom) air supply, CO and C_xH_y at the secondary combustion zone and upper regions inside the reactor increase, facilitating a noticeable reduction of NO in these regions and resulting, consequently, in lower NO emission from the combustor. However, the co-firing method causes some deterioration of the combustion efficiency of the reactor. The best combustion and emission performance of the conical FBC can be achieved when co-firing pelletized rice husk and moisturized rice husk at the 15% energy contribution by the secondary fuel to the reactor heat input and ~40% excess air, ensuring high (~99%) combustion efficiency at minimal emission (or "external") costs of the reactor. With these optimal operating parameters, the NO emission can be reduced by ~40% compared to the individual burning of rice husk pellets, while controlling CO and C_xH_y emissions from the combustor at acceptable levels.

5. Acknowledgements

The authors would like to acknowledge the financial support from the National Research Council of Thailand and from the Thailand Research Fund.

6. References

[1] Office of Agricultural Economics, Ministry of Agriculture and Cooperatives; Thailand. URL: http://www.oae.go.th/production.html, assessed on 31/10/2016.

[2] Department of Alternative Energy Development and Efficiency, Ministry of Energy, Thailand. Thailand alternative energy situation 2014. URL: http://www4.dede.go.th/dede/images/stories/stat_dede/sit_58/Thailand%20Alternative%20Energy%20Situation%202014.pdf, assessed on 31/10/2016.

[3] Fang, M., Yang, L., Chen, G., Shi, Z., Luo, Z., and Cen, K. (2004). Experimental study on rice husk combustion in a circulating fluidized bed. *Fuel Processing Technology*, vol. 85(11), August 2004, pp. 1273–1282.

[4] Kuprianov, V.I., Kaewklum, R., Sirisomboon, K., Arromdee, P., and Chakritthakul, S. (2010). Combustion and emission characteristics of a swirling fluidized-bed combustor burning moisturized rice husk. *Applied Energy*, vol. 87(9), September 2010, pp. 2899–2906.

[5] Werther, J., Saenger, M., Hartge, E.-U., Ogada, T., and Siagi, Z. (2000). Combustion of agricultural residues. *Progress in Energy and Combustion Science*, vol. 26(1), February 2000, pp. 1–27.

[6] Madhiyanon, T., Sathitruangsak, P., and Soponronnarit, S. (2010). Combustion characteristics of rice-husk in a short-combustion-chamber fluidized-bed combustor (SFBC). *Applied Thermal Engineering*, vol. 30(4), March 2010, pp. 347–353.

[7] Sirisomboon, K., Kuprianov, V.I., and Arromdee, P. (2010). Effects of design features on combustion efficiency and emission performance of a biomass-fuelled fluidized-bed combustor. *Chemical Engineering and Processing: Process Intensification*, vol. 49(3), March 2010, pp. 270-277.

[8] Nussbaumer, T. (2003). Combustion and co-combustion of biomass: fundamentals, technologies, and primary measures for emission reduction. *Energy & Fuels*, vol. 17(6), November 2003, pp. 1510–1521.

[9] Sami, M., Annamalai, K., and Wooldridge, M. (2001). Co-firing of coal and biomass fuel blends. *Progress in Energy and Combustion Science*, vol. 27(2), pp. 171–214.

[10] Kuprianov, V.I., Janvijitsakul, K., and Permchart, W. (2006). Co-firing of sugar cane bagasse with rice husk in a conical fluidized-bed combustor. *Fuel*, vol. 85(4), March 2006, pp. 434–442.

[11] Chakritthakul, S. and Kuprianov, V.I. (2011). Co-firing of eucalyptus bark and rubberwood sawdust in a swirling fluidized-bed combustor using an axial flow swirler. *Bioresource Technology*, vol. 102(17), September 2011, pp. 8268–8278.

[12] Baukal, C.E.(Jr.). (2001). The John Zink Combustion Handbook, CRC Press, New York.

[13] Suheri, P. and Kuprianov, V.I. (2015). Co-firing of oil palm empty fruit bunch and kernel shell in a fluidized-bed combustor: Optimization of operating variables. *Energy Procedia*, vol. 79, November 2015, pp. 956–962.

[14] Madhiyanon, T., Sathitruangsak, P., and Soponronnarit, S. (2009).Co-combustion of rice husk with coal in a cyclonic fluidized-bed combustor (ψ-FBC). *Fuel*, vol. 88(1), January 2009, pp. 132-138.

[15] Visser, H.J.M., Van Lith, S.C., and Kiel, J.H.A. (2008). Biomass ash-bed material interactions leading to agglomeration in FBC. *Journal of Energy Resources Technology, Transactions of the ASME*, vol. 130(1), January 2008, pp. 118011–118015.

[16] Ninduangdee, P. and Kuprianov, V.I. (2016). A study on combustion of oil palm empty fruit bunch in a fluidized bed using alternative bed materials: Performance, emissions, and time-domain changes in the bed condition. *Applied Energy*, vol. 176, August 2016, pp. 34–48.

[17] Ninduangdee, P. and Kuprianov, V.I. (2014). Combustion of palm kernel shell in a fluidized bed: Optimization of biomass particle size and operating conditions. *Energy Conversion and Management*, vol.85, September 2014, pp. 800-808.

[18] Basu, P., Cen, K.F., and Jestin, L. (2000). Boilers and Burners, Springer, New York.

[19] Kuprianov, V.I., Kaewklum, R., Chakritthakul, S. (2011). Effects of operating conditions and fuel properties on emission performance and combustion efficiency of a swirling fluidized-bed combustor fired with a biomass fuel. *Energy*, vol. 36(4), April 2011, pp. 2038–2048.

[20] ESCAP-UN. (1995). Energy efficiency, United Nations, New York.

[21] Wei, X., Zhang, L., and Zhou, H. (2003). Evaluating the environmental value of pollutants in China power industry, paper presented *in the International Conference on Energy and the Environment*, Shanghai, China.

[22] Turns, S. (2006). An introduction to Combustion, McGraw-Hill, Boston.

[23] Winter, F., Wartha, C., and Hofbauer, H. (1999). NO and N_2O formation during the combustion of wood, straw, malt waste and peat. *Bioresource Technology*, vol. 70(1), October 1999, pp. 39–49.